

Supplement of *Clim. Past*, 10, 1581–1601, 2014
<http://www.clim-past.net/10/1581/2014/>
doi:10.5194/cp-10-1581-2014-supplement
© Author(s) 2014. CC Attribution 3.0 License.



Supplement of

Expressions of climate perturbations in western Ugandan crater lake sediment records during the last 1000 years

K. Mills et al.

Correspondence to: K. Mills (k.mills2@lboro.ac.uk)

1 Mills et al – Supplementary Material

2 1 Results

3 1.1 Core correlation and chronological analyses

4 1.1.1 Lake Nyamogusingiri

5 *Core correlation.* Four cores were collected from Lake Nyamogusingiri: two Kajak cores
6 (NCR1 0-29 cm; NCR2 0-35 cm) and two Russian cores (NCR1C1 0-85 cm; NCR2C1 0-100
7 cm). Only the longer Kajak core (NCR2) was used for analysis as it provided a larger overlap
8 with the top of the Russian cores (8 cm). During the retrieval of core NCR1C1 the core
9 chamber failed to close correctly and sediments were lost. As the integrity of this core was
10 compromised NCR1C1 was not considered for analysis. The second core drive (NCR2C1)
11 was successful and selected for analysis.

12 Due to the lack of any obvious defining stratigraphic or sedimentological indicators (e.g.
13 banding) in the Nyamogusingiri cores, cores were first correlated on the basis of the field
14 calculations of the coring depths. This correlation was subsequently corrected and finalised
15 based on the loss-on-ignition and diatom analysis (Figure S1), with *Thalassiosira rudolfi*
16 being a key species in the confirmation of the overlap (Figure 4a, main text). The composite
17 core length for Lake Nyamogusingiri was 1.27 m.

18 *Chronological analysis.* ^{210}Pb activity in Nyamogusingiri reaches equilibrium with the
19 supporting ^{226}Ra at a depth of c. 50 cm. The unsupported ^{210}Pb activity declines steeply and
20 almost exponentially with depth in the upper 10 cm, but at a slower rate than in deeper
21 sections (Figure S2a-d). This gradient change indicates a recent reduction in the
22 sedimentation rate, but may also be attributed to the shift to lower density sediments in the
23 upper 10 cm of the core.

24 The ^{137}Cs activity shows a relatively well-defined peak at 20-26 cm (Figure S2a-d) and almost
25 certainly records the 1963 fallout maximum from the atmospheric testing of nuclear weapons
26 (P.G. Appleby, pers. comm.). The ^{210}Pb chronology for Nyamogusingiri places 1963 at 27
27 cm, a little below the depth indicated by the ^{137}Cs record. The revised dates were calculated
28 by applying the constant rate of supply (CRS) model (Appleby and Oldfield, 1978) in a
29 piecewise way using the 1963 ^{137}Cs date as a reference point. The results suggest a relatively

1 high sedimentation rate from c. AD 1930 through to the early 1990s, with peak values
2 occurring in the mid-1940s and mid-1980s (P.G. Appleby, pers. comm.).

3 Five AMS ^{14}C dates were obtained from Lake Nyamogusingiri's composite core sequence,
4 below the ^{210}Pb equilibrium depth (c. 52 cm). Two dates from near the base of the core
5 sequence were rejected (Table 1, main text); the dates for these lower samples were obtained
6 on two wood/charcoal fragments and produced younger radiocarbon ages, and hence a
7 younger calibrated date compared to the other three dates above, which all occurred in
8 stratigraphic sequence.

9 The young ages of SUERC-18396 (wood) and POZ-26361 (charcoal) were both rejected from
10 the final age model. The young age of SUERC-18396 indicate an intrusive root fragment
11 during a period of lower lakes levels (Krider, 1998), especially as the sample was extracted
12 from a soil like deposit at the base of the core. It is worth noting that both of these samples
13 overlap at the 2-sigma confidence limit and also overlap with the date obtained at 61 cm. It
14 may therefore be plausible that during coring the nose or blade of Russian corer dragged
15 down younger material, causing modern contamination of older sediments.

16 **1.1.2 Lake Kyasanduka**

17 *Core correlation.* Six cores were collected from Lake Kyasanduka: two Kajak cores (KYAS-
18 1; core length 0-39 cm; KYAS-2 0-28 cm) and four Russian cores (KR1C1 31-99 cm; KR2C1
19 20-100 cm; KR1C2 4-97 cm and KR2C2 0-100 cm; 0 cm represents the top of the Russian
20 Core chamber; 100 cm is the base of the chamber. Where sediment was not retrieved, the top
21 of the core represents the depth where the intact sediment core begins). Preliminary core
22 correlations were made using the field notes related to coring depths. Detailed core
23 correlations were completed through the use of the core descriptions, loss-on-ignition (organic
24 content) profiles, magnetic susceptibility profiles and high-resolution diatom analysis on
25 overlapping sections.

26 Core descriptions made in the field immediately after collection and the supplementary
27 descriptions taken in the laboratory identified several laminated sections in all four of the
28 Russian cores. These sections of banding provided a key tool for the visual correlation of the
29 four core sequences (Figure S2). They included a section of discontinuous banding in the
30 middle of KR2C1 (c. 45-50 cm) which was correlated with a thin black band in KR1C1 (at c.
31 85 cm). A section of banding consisting of orange, brown, red and grey laminations was

1 identified at the base of KR2C1 (80-84 cm) and the upper sections of KR1C2 and KR2C2
2 (14-18 cm and 14-17 cm), providing a clear tie point for the correlation of these lower core
3 sequences.

4 The correlations based on the core stratigraphy were confirmed by the loss-on-ignition
5 analyses (organic content) and the magnetic susceptibility. However, the lower sections of the
6 sequence (KR1C2 and KR2C2) were more difficult to correlate, due to several deviations in
7 the organic content and magnetic susceptibility. However, detailed diatom analyses (Figure
8 S3) revealed an almost identical stratigraphy in both cores. Using key features from the cores
9 the offset between the accumulation rates in the two cores, the KR2C2 sequence was
10 stretched relative to KR1C2, following Shaw (1964; Figure S3). The adjustment of the
11 KR2C2 record resulted in the composite core sequence being 2.17 m in length.

12 *Chronological analysis.* The ^{210}Pb inventory from Lake Kyasanduka is not comparable to the
13 value supported by the atmospheric flux (6463 Bq m^{-2}); rather it is double the fallout value
14 (16082 Bq m^{-2} ; P.G. Appleby, *pers. comm.*). This high value may be the result of strong
15 sediment focusing at the core site, or significant inputs via catchment erosion. As a large part
16 of the lake's catchment lies outside of the Central Forest Reserve boundary, which is subject
17 to large-scale clearance of natural vegetation for subsistence agriculture, the high value is
18 most likely attributed to significant inputs as a result of catchment erosion.

19 Kyasanduka has a number of irregularities in its unsupported ^{210}Pb activity (Figure S3a-d)
20 suggesting several periods of major disturbances in the recent past. Total ^{210}Pb reaches
21 equilibrium with the supporting ^{226}Ra at a depth of around 125 cm. ^{210}Pb concentrations have
22 a maximum value 8.5 cm below the top of the core and there is a further significant non-
23 monotonic feature between 24 and 50 cm. The presence of a layer of dense sediment between
24 120 and 140 cm may be related to the virtual absence of unsupported ^{210}Pb below 110 cm.
25 This dense sediment is interpreted as a large, simultaneous deposit of catchment material that
26 may have caused dilution of the ^{210}Pb concentrations in the lake sediments.

27 The ^{137}Cs activity versus depth profile of Kyasanduka shows a peak between 44 cm and 53
28 cm but as rapid changes in ^{210}Pb occur at the same interval in the core, but radiocaesium is
29 present to c. 70 cm in the core and it is likely that the factors driving these changes have also
30 modified the ^{137}Cs profile (P.G. Appleby, *pers. comm.*). Thus a more appropriate guide to the
31 1963 depth may be obtained by using the $^{137}\text{Cs}/^{210}\text{Pb}$ ratio (which peaks at 38-49 cm).

1 Figure S3a shows the ^{210}Pb dates calculated using the CRS model, together with the 1963
2 depth suggested by the ^{137}Cs record. Use of the constant initial concentration (CIC) model
3 was precluded by the irregular nature of the ^{210}Pb record. The ^{210}Pb results place 1963 at
4 ca.60 cm, significantly below the depth indicated by the ^{137}Cs record. The discrepancy
5 appears to be due to changes in the ^{210}Pb supply rate to the sediments associated with the
6 irregularities in the sediment record. Calculations using the ^{137}Cs date as a reference point
7 indicate that the very high ^{210}Pb inventory in this core is mainly attributable to very high
8 supply rates in the pre-1963 period. The mean post-1963 ^{210}Pb flux ($\sim 350 \text{ Bq m}^{-2} \text{ y}^{-1}$) is less
9 than 40% of the value ($\sim 950 \text{ Bq m}^{-2} \text{ y}^{-1}$) calculated for the pre-1963 sediments. Revised dates
10 calculated by applying the CRS model in a piecewise way using the 1963 ^{137}Cs date as a
11 reference point suggest a relative uniform sedimentation rate of around $0.047 \text{ g cm}^{-2} \text{ y}^{-1}$ (0.60-
12 0.90 cm y^{-1}) since the later part of the 19th century, punctuated by episodes of rapid
13 accumulation in the 1920s, the late 1960s or early 1970s, and most recently during the past
14 few years.

15 Eleven AMS ^{14}C dates on terrestrial material (leaves, wood, and charcoal) were obtained Lake
16 Kyasanduka's composite core sequence. All dates were calibrated using CALIB 5.0 (Stuiver
17 and Reimer, 1993) using the IntCal09 calibration curve (Reimer et al., 2009). Out of the
18 eleven dates, three were rejected (Table 1, main text): SUERC-19070 (charcoal), SUERC-
19 18398 (charred wood) and POZ-26360 (charcoal). Whilst the pure charcoal and charred wood
20 fragments selected for analysis were $>250 \mu\text{m}$ in length, suggesting a local source, and those
21 with rounded edges were avoided to try and limit errors due to the reworking of charcoal in
22 the sediments, the dates all produced consistently older ages than the sediments dated above
23 and below, or in the case of SUERC-19065, the charcoal date produced an older age than a
24 second date obtained from the same horizon from a piece of wood. These older charcoal ages
25 could be due to 'old wood' (containing old carbon) having been partially burned and
26 deposited in the lake, or the reworking of older charcoal remaining within the catchment and
27 was deposited in the lake during periods of high sedimentation as a result of rainfall events or
28 catchment disturbance. It should be noted that not all dates obtained on charcoal were
29 rejected. The accepted dates were those where more brittle terrestrial plant material (e.g. leaf
30 fragments) and smaller pieces of wood and charcoal ($<250 \mu\text{m}$). These more delicate plant
31 fragments would likely be destroyed by prolonged aerial exposure. Furthermore, when such
32 remains are found in offshore sediments, they most likely reflect direct deposition from the air
33 (Verschuren, 2003).

1 Problems with the dating of charcoal, which appear older when compared to other dates
2 above and below the charcoal date, in the East African crater lakes has been reported (Russell
3 et al., 2007), yet the occurrence of terrestrial macrofossils in these cores was rare, limiting the
4 available material for dating. Dating of bulk sediment samples is not optimal in these closed
5 crater lakes, as bulk samples have been older than expected, interpreted as a result of carbon
6 reservoir effect (Beuning et al., 1997; Stager and Johnson, 2000; Russell et al., 2007). The
7 dating of bulk sediments in some of the larger and smaller (crater) lakes in East Africa has
8 proved problematic. In many instances, bulk sedimentary material may contain considerable
9 ^{14}C from aquatic algae, which can overestimate the true age of the sediment. Aquatic algae
10 derive their ^{14}C from the dissolved inorganic carbon from the lake water, and in many closed-
11 basin lakes, the long residence time can cause a reduction in the $^{14}\text{C}/^{12}\text{C}$ ratio relative to the
12 atmosphere (Verschuren, 2003). For example, radiocarbon dated sediments from Lake
13 Victoria suggest a 500-600 year offset in core tops (Beuning et al., 1997; Stager and Johnson,
14 2000).

15

16 **1.2 Other considerations**

17 *Sediment disturbance:* Whilst Lake Kyasanduka is a shallow lake system (whose maximum
18 depth is restricted to 3 m due to an overflow and sediment infilling), there is little evidence in
19 both the diatom stratigraphy and in the sedimentology that suggest wind-mixing/bioturbation
20 is not a major issue for this system. With regards to the biostratigraphy, there are no clear
21 signs of mixing within the diatom stratigraphy many of the changes between distinct habitat
22 groups are very clear, and there is little in the way of evidence of the mixing of signals of
23 different diatom groupings (at the resolution of these analyses). The catchment of Lake
24 Kyasanduka, whilst not having high crater sides, is relatively sheltered by high ground to the
25 east and dense vegetation that surrounds the lake. Limnological profiles in terms of
26 temperature and chemistry were also recorded during the day and show clear stratification,
27 suggesting that, during the dry season at least, wind mixing is not prevalent.

28 *Chronological uncertainty:* There may be additional chronological uncertainty in the age
29 models from Lakes Kyasanduka and Nyamogusingiri due to the occurrence of non-unique
30 calendar ages (Verschuren et al., 2000). The calculation of the calendar ages is particularly
31 problematic during the last 1000 years due to the 'de Vries effect', which causes several
32 plateaus as well as age reversals in the radiocarbon calibration. This results in multiple

1 calibrated ages for single samples (Table 1, main text). The de Vries effect is a natural
2 phenomenon often linked to variations in sunspot activity, which can cause problems with the
3 precision of calibrated radiocarbon dates from AD 1450 to AD 1950 (Stuiver and Becker,
4 1993). In some instances these perturbations can cause limitations when resolving the actual
5 ages of the sediments.

6

7 **References**

- 8 Appleby, P. G. and Oldfield, F.: The calculation of ^{210}Pb dates assuming a constant rate of
9 supply of unsupported ^{210}Pb to the sediment, *Catena*, 5, 1-8, 1978.
- 10 Beuning, K. R. M., Talbot, M. R. and Kelts, K.: A revised, 30,000-year palaeoclimatic and
11 paleohydrologic history of Lake Albert, East Africa, *Palaeogeogr. Palaeoclimatol.*
12 *Palaeoecol.*, 136, 259-279, 1997.
- 13 Krider, P.R.: Paleoclimatic significance of Late Quaternary lacustrine and alluvial
14 stratigraphy, Animas Valley, New Mexico, *Quat. Res.*, 50, 283-289, 1998.
- 15 Mills, K. Ugandan Crater Lakes: Limnology, Palaeolimnology and Palaeoenvironmental
16 History. Ph. D. thesis, Loughborough University, 429 pp., 2009.
- 17 Moy, C. M., Seltzer, G., Rodbell, D. T. and Anderson, D. M.: Variability of El Niño/Southern
18 Oscillation activity at millennial timescales during the Holocene epoch, *Nature*, 404, 162-165,
19 2002.
- 20 Reimer, P. J., Baillie, M. G. L., Bard, E., Bayliss, A., Beck, J. W., Blackwell, P. G., Bronk
21 Ramsey, C., Buck, C. E., Burr, G. S., Edwards, R. L., Friedrich, M., Grootes, P. M.,
22 Guilderson, T. P., Hajdas, I., Heaton, T. J., Hogg, A. G., Hughen, K. A., Kaiser, K. F.,
23 Kromer, B., McCormac, F. G., Manning, S. W., Reimer, R. W., Richards, D. A., Southon, J.
24 R., Talamo, S., Turney, C. S. M., van der Plicht, J. and Weyhenmeyer, C. E.: INTCAL09 and
25 MARINE09 radiocarbon age calibration curves, 0-50,000 years cal BP, *Radiocarbon*, 51,
26 1111-1150, 2009.
- 27 Russell, J. M. and Johnson, T. C.: Little Ice Age drought in equatorial Africa: Intertropical
28 Convergence Zone migrations and El Niño-Southern Oscillation variability. *Geol. Soc. Am.*,
29 35, 21-24, 2007.

- 1 Russell, J.M., Eggermont, H., Verschuren, D. (2007). Spatial complexity during the Little Ice
2 Age in tropical East Africa: sedimentary records from contrasting crater lake basins in
3 western Uganda. *The Holocene* **17**: 183-193.
- 4 Ryves, D. B., Mills, K., Bennike, O., Brodersen, K. P., Lamb, A. L., Leng, M. J., Russell, J.
5 M. and Ssemmanda, I.: Environmental change over the last millennium recorded in two
6 contrasting crater lakes in western Uganda, eastern Africa (Lakes Kasenda and Wandakara),
7 *Quat. Sci. Rev.*, **30**, 555-569, 2011.
- 8 Shaw, A. B.: *Time in Stratigraphy*. McGraw-Hill, New York, 1964.
- 9 Stager, J. C., Johnson, T. C.: A 12,400 ¹⁴C yr offshore diatom record from east central Lake
10 Victoria, East Africa, *J. Paleolimnol.*, **23**, 373-383, 2000.
- 11 Stager, J. C., Ryves, D., Cumming, B. F., Meeker, L. D. and Beer, J.: Solar variability and the
12 levels of Lake Victoria, East Africa, during the last millennium, *J. Paleolimnol.*, **33**, 243-251,
13 2005.
- 14 Stuiver, M. and Becker, B.: High-precision decadal calibration of the radiocarbon timescale,
15 AD 1950-6000 BC, *Radiocarbon*, **35**, 35-65, 1993.
- 16 Stuiver, M. and Reimer, P. J.: Extended ¹⁴C database and revised CALIB radiocarbon
17 calibration program, *Radiocarbon* **35**, 215-230, 1993.
- 18 Solanki, S. K., Usoskin, I. G., Kromer, B., Schüssler, M. and Beer, J.: Unusual activity of the
19 Sun during recent decades compared to the previous 11,000 years, *Nature*, **431**, 1084-1087,
20 2004.
- 21 Verschuren, D.: Reconstructing fluctuations of a shallow East African lake during the past
22 1800 years from sediment stratigraphy in a submerged crater basin, *J. Paleolimnol.*, **25**, 297-
23 311, 2001.
- 24 Verschuren, D.: Lake-based climate reconstruction in Africa: progress and challenges,
25 *Hydrobiologia*, **500**, 315-330, 2003.
- 26 Verschuren, D., Laird, K. R. and Cumming, B. F.: Rainfall and drought in equatorial east
27 Africa during the past 1,100 years, *Nature*, **403**, 410-414, 2000.

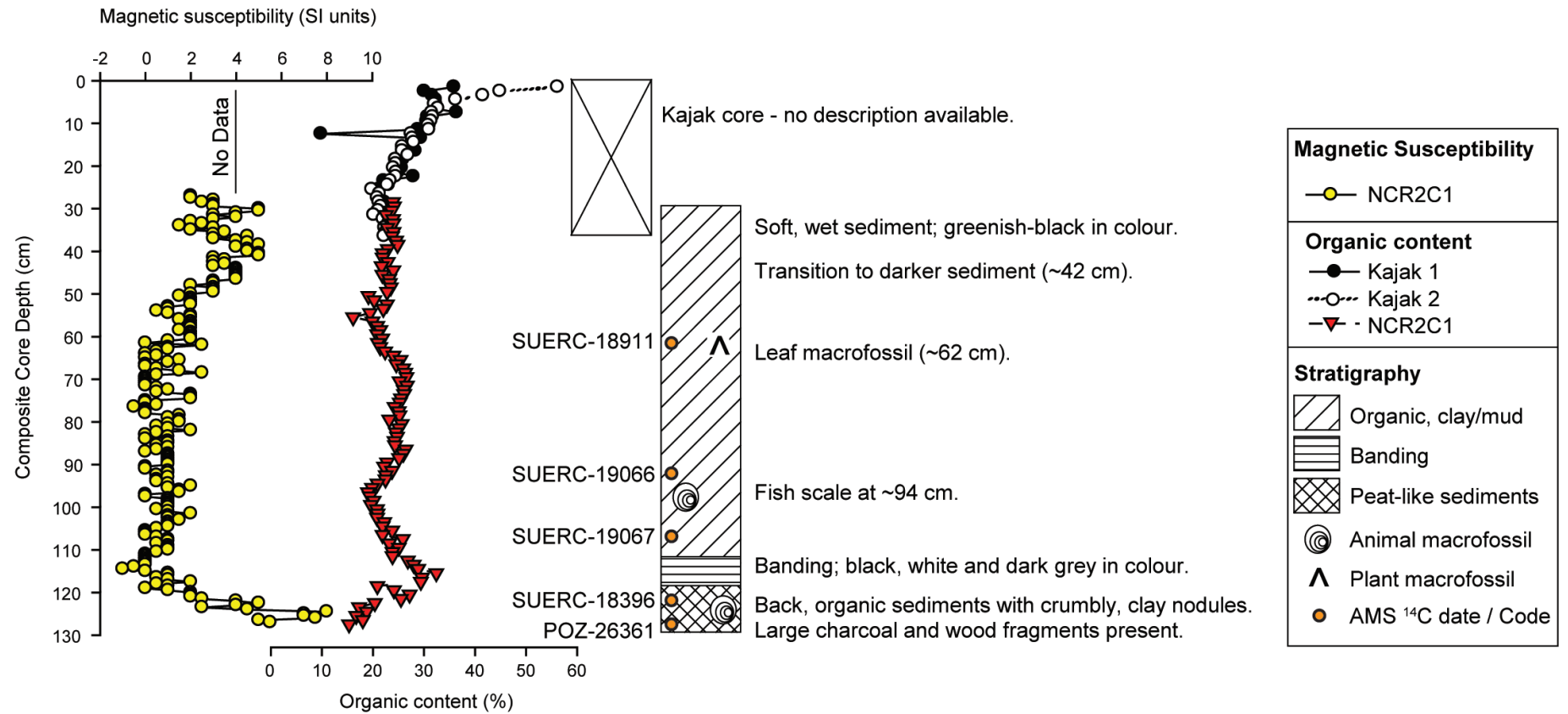
1 Table S1. Variables used in the RDA prior to forward selection of the statistically significant
 2 variables for each core

3

Variable	Description	Reference
LOCAL DRIVERS		
DMAR	Dry mass accumulation rate ($\text{g cm}^2 \text{yr}^{-1}$)	Mills, 2009
Organic flux	Calculated flux rate of organic matter (LOI)	Mills, 2009
Minerogenic flux	Calculated flux rate of minerogenic matter (LOI)	Mills, 2009
$\delta^{13}\text{C}_{\text{org}}$	Bulk organic isotope data	Mills, 2009
CN ratio	Carbon: nitrogen ratio (bulk sediments)	Mills, 2009
REGIONAL DRIVERS		
Lake Pallcacocha	ENSO frequency (red colour intensity)	Moy et al., 2002
Atmospheric $\delta^{14}\text{C}$ residual series	Relationship to sunspot minima	Stuiver and Brauzanias, 1989
Lake Naivasha	Reconstructed lake level (m)	Verschuren et al. 2000
Lake Edward	Mg in calcite (%)	Russell and Johnson, 2007
Lake Victoria	Shallow water diatoms (% SWD)	Stager et al., 2005
Lake Kibengo	CaCO_3 (%)	Russell et al., 2007
Lake Kitagata	Magnetic susceptibility (SI Units)	Russell et al., 2007
Lake Kasenda	Inferred lake level	Ryves et al., 2011

4

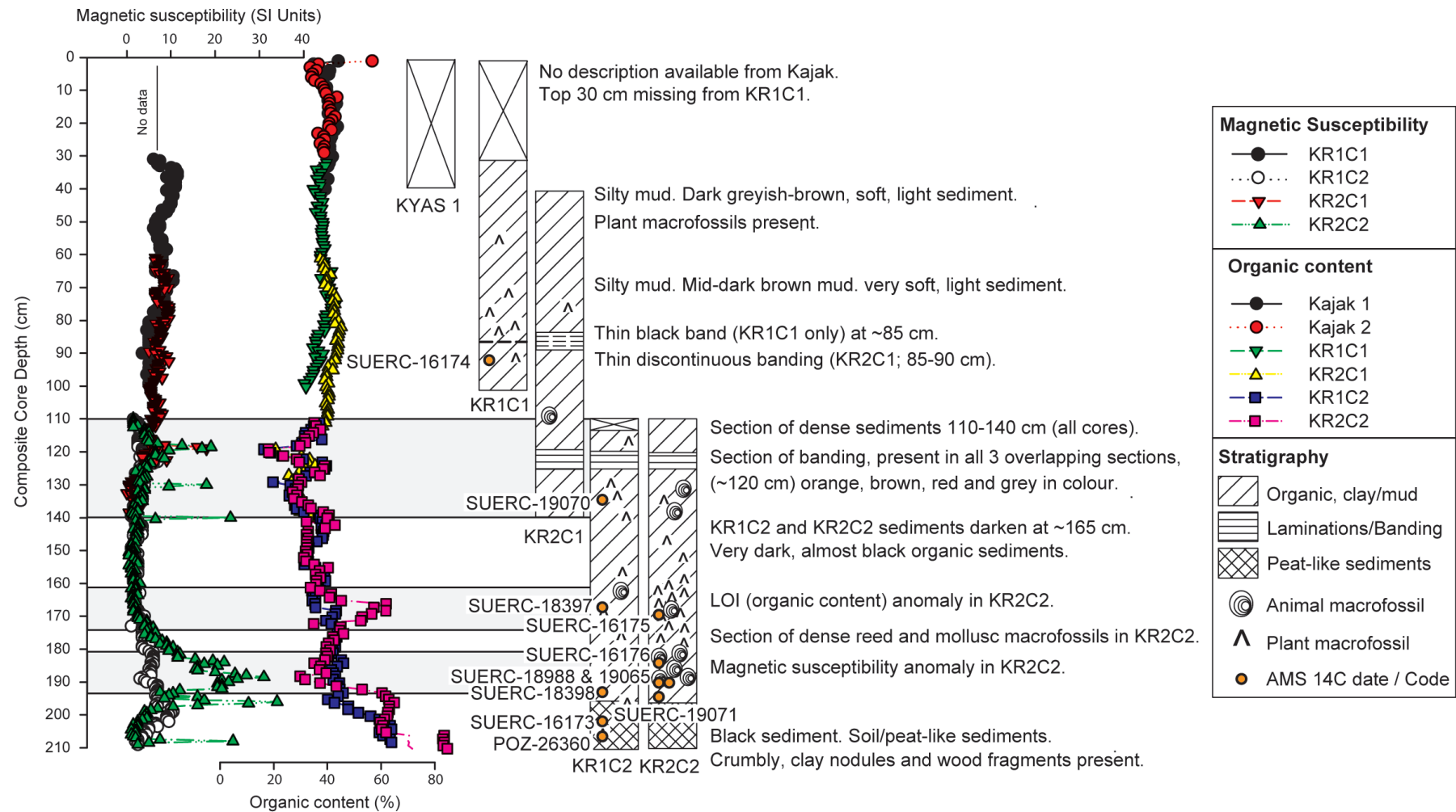
1



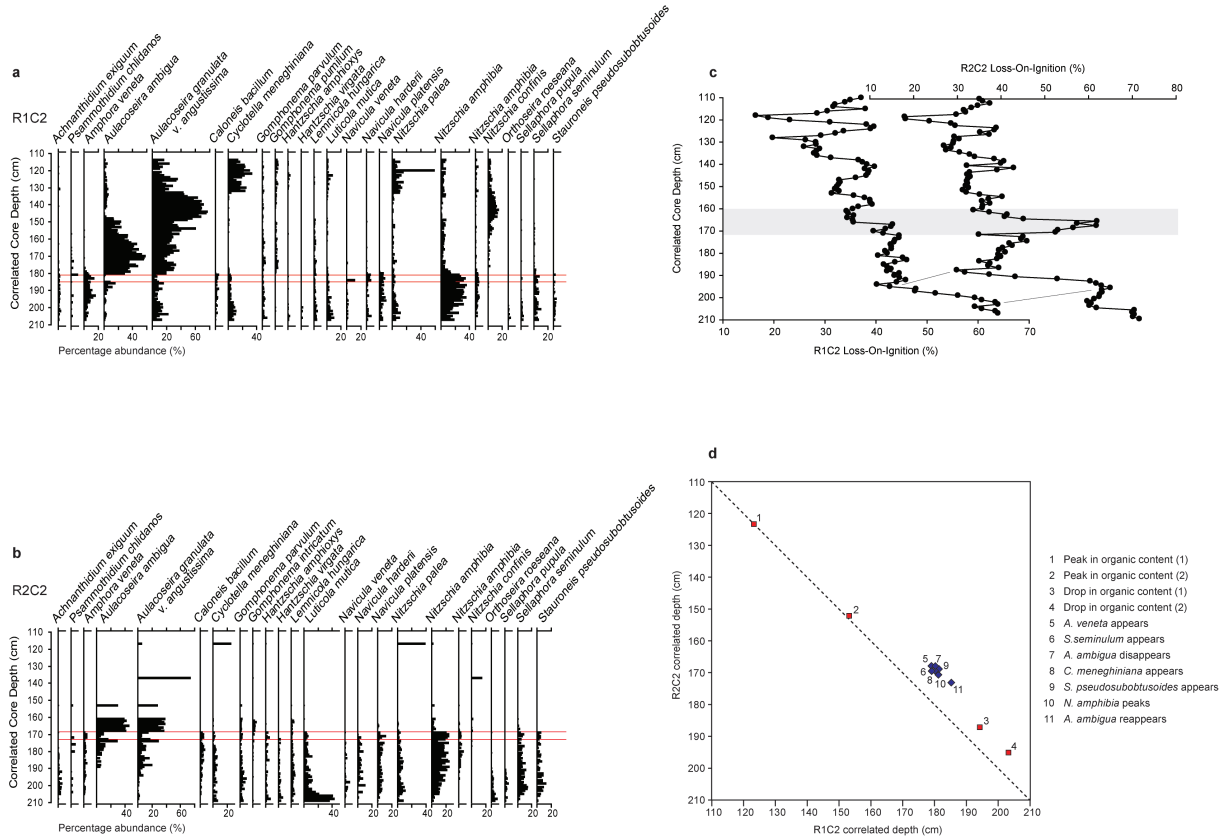
2

3

4 Figure S1. Correlation of the overlapping core sections recovered from Lake Nyamogusingiri. Results of magnetic susceptibility, loss-on-
 5 ignition and core stratigraphies are displayed alongside brief descriptions.



1
 2 Figure S2. Correlation of the overlapping core sections recovered from Lake Kyasanduka. Results of magnetic susceptibility, loss-on-ignition
 3 and core stratigraphies are displayed alongside brief descriptions.



2

3

4 Figure S3. Detailed diatom counts from Kyasanduka cores (a) KR1C2 and (b) KR2C2. The
 5 red boundaries highlight the key feature (a reduction in the percentage of *Aulacoseira* species)
 6 that was used to confirm the core correlation, (c) loss-on-ignition profiles of cores KR1C2
 7 and KR2C2. The shaded box indicates the excursion in the LOI profile as noted in KR2C2
 8 only, which corresponds to a reed mat deposit in the core and (d) Shaw diagram for the
 9 overlapping cores KR1C2 and KR2C2. Each point (1-11) represents an assumed synchronous
 10 feature, derived using loss-on-ignition and diatom biostratigraphy. The deviation from the 1:1
 11 line towards the bottom of both cores suggests a change in sedimentation rate between the
 12 two cores and their depositional environments.